The table shows that for a probability of a binary one due to noise of .2625, Equation D-22 is satisfied. That is, the peak noise level will be approximately one volt if the threshold comparator is set for P_{N1} = .2625. Therefore, using Figure D-35, the threshold comparator threshold-to-rms noise (T/N) ratio should be set at 1.5 dB for the MTI channel and 4.25 dB for the normal channel.

TABLE D-4 shows the probability of the binary counter reaching each state due to noise, P_{nj}, and the cumulative probability of P_{nj} for the FAA modified integrator and P_{N1} of 10^{-2}, 10^{-1}, and .135. The table shows that a threshold comparator setting of P_{N1} = .135 will limit the peak noise level to approximately one volt. That is, Equation D-22 is satisfied for a P_{N1} of .135. Again, using Figure D-35, the threshold comparator T/N ratio should be set for the FAA modified integrator at 3.2 dB for the MTI channel and 6.0 dB for the normal channel.

TABLE D-5 shows the probability of the binary counter reaching each state due to noise, P_{nj}, and the cumulative probability of P_{nj} for a computer simulation of the enhancer hardware (see Appendix E). The simulated run was for a threshold comparator setting of P_{N1} = .2625 (same as in TABLE D-3). Only one thousand noise samples were taken. Therefore, the probability of being in each state, P_{nj}, will only be accurate for $P_{nj} > .005$. TABLE D-5 compares favorably with TABLE D-3, thus validating Equation D-20b.

Desired Signal

For a nonfluctuating target (Marcum's Case 0), the probability of the desired signal exceeding the threshold comparator level (P_{S1} probability for a binary one in a range bin) for the normal channel has a Rice (1954) PDF (also known as the Modified Rayleigh and Q-function).

$$P_{S1} = \int_T^{\infty} \frac{ve}{\sigma^2}^{\frac{-(v^2+A^2)}{2\sigma^2}} I_o\left(\frac{vA}{\sigma^2}\right) dv \qquad \text{(D-23)}$$

where:

I_o ( ) = Modified Bessel function of the first kind of order zero

A = Peak signal-amplitude, in volts

σ = rms noise level, in volts

T = Threshold comparator threshold level, in volts

The integrand of Equation D-23 is the signal-plus-noise amplitude distribution at the threshold comparator input for the normal or dual MTI channel (see Figure 3-10). Figure D-36 shows the probability of the desired signal-plus-noise exceeding the threshold comparator level (P_{S1}, probability

TABLE D-4

PROBABILITY OF NOISE CAUSING THE MODIFIED FAA INTEGRATOR TO BE IN STATE E_j

State E_j	Counter Level	$P_{N1} = 10^{-2}$	
		P_{nj}	ΣP_{nj}
1	0	.989898990+000	.989898990+000
2	1	.999897957-002	.999897970+000
3	2	.100999792-003	.999998969+000
4	4	.102019991-005	.999999990+000
5	8	.103050495-007	.100000000+001
6	16	.104091408-009	.100000000+001
7	31	.105142835-011	.100000000+001

State E_j	Counter Level	$P_{N1} = 10^{-1}$	
		P_{nj}	ΣP_{nj}
1	0	.888889077+000	.888889077+000
2	1	.987654512-001	.987654528+000
3	2	.109739388-001	.998628467+000
4	4	.121932652-002	.999847793+000
5	8	.135480722-003	.999983274+000
6	16	.150534132-004	.999998327+000
7	31	.167260144-005	.100000000+001

State E_j	Counter Level	$P_{N1} = .135$	
		P_{nj}	ΣP_{nj}
1	0	.843932543+000	.843932543+000
2	1	.131712012+000	.975644555+000
3	2	.205562096-001	.996200765+000
4	4	.320819449-002	.999408959+000
5	8	.500700862-003	.999909660+000
6	16	.781440635-004	.999987804+000
7	31	.121958940-004	.100000000+001

TABLE D-5

PROBABILITY OF NOISE CAUSING THE
INTEGRATOR TO BE IN STATE E_j (SIMULATED)

State E_j	Counter Level	$P_{N1} = .2625$	
		P_{nj}	ΣP_{nj}
1	0	.632103689+000	.632103689+000
2	1	.235294118+000	.867397807+000
3	2	.867397807-001	.954137587+000
4	3	.329012961-001	.987038883+000
5	4	.109670987-001	.998005982+000
6	5	.199401795-002	.100000000+001
7	6	.000000000	.100000000+001
8	7	.000000000	.100000000+001
9	8	.000000000	.100000000+001
10	9	.000000000	.100000000+001
11	10	.000000000	.100000000+001
12	11	.000000000	.100000000+001
13	12	.000000000	.100000000+001
14	13	.000000000	.100000000+001
15	14	.000000000	.100000000+001
16	15	.000000000	.100000000+001
17	16	.000000000	.100000000+001
18	17	.000000000	.100000000+001
19	18	.000000000	.100000000+001
20	19	.000000000	.100000000+001
21	20	.000000000	.100000000+001
22	21	.000000000	.100000000+001
23	22	.000000000	.100000000+001
24	23	.000000000	.100000000+001
25	24	.000000000	.100000000+001
26	25	.000000000	.100000000+001
27	26	.000000000	.100000000+001
28	27	.000000000	.100000000+001
29	28	.000000000	.100000000+001
30	29	.000000000	.100000000+001
31	30	.000000000	.100000000+001
32	31	.000000000	.100000000+001

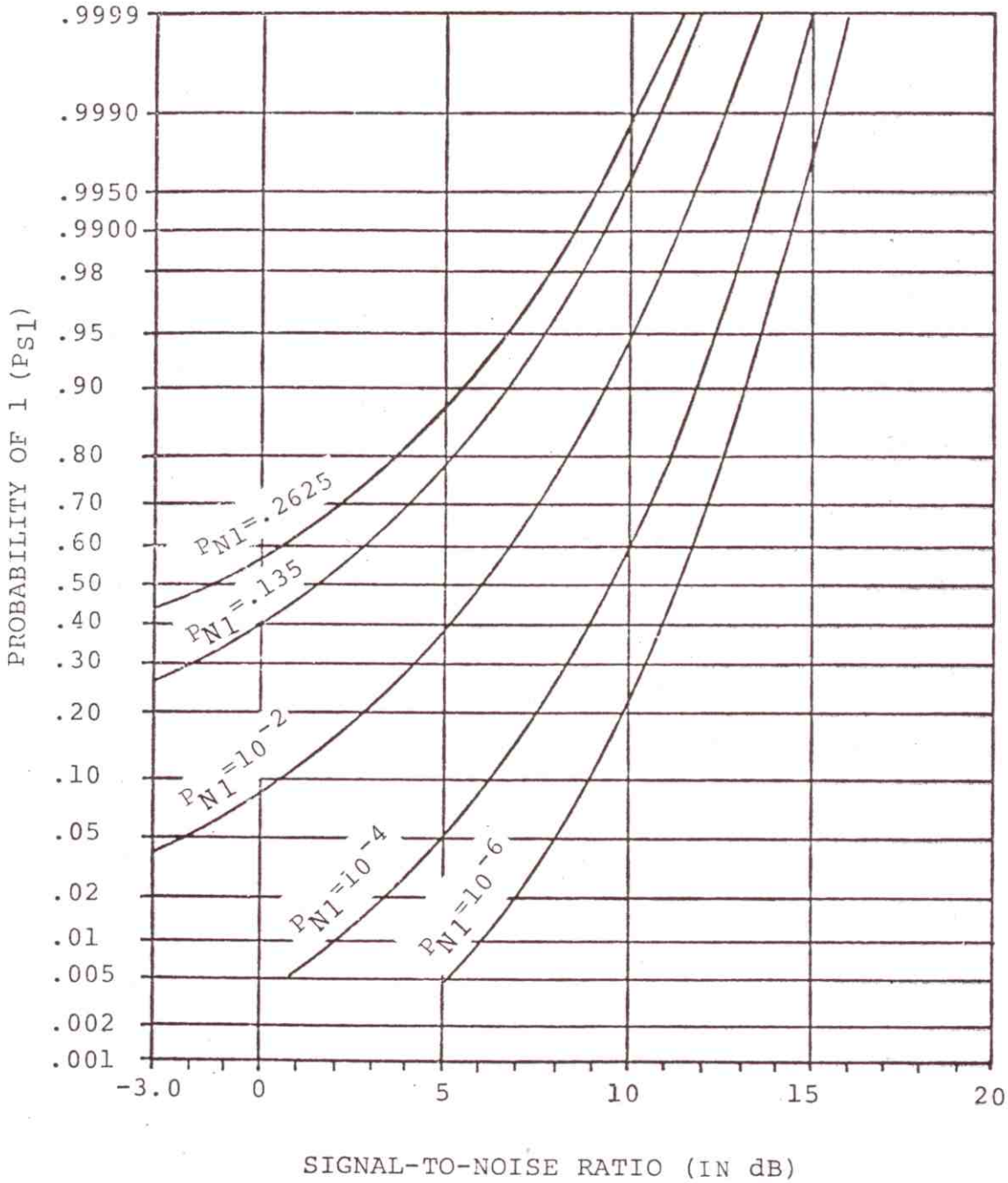

Figure D-36. Probability of 1 at the Threshold Comparator Output as a Function of the Signal-to-Noise Ratio at the threshold Comparator Input for the Normal Channel.

of a binary one in a range bin). The probability of exceeding the threshold comparator level, P_{S1}, is shown as a function of the signal-to-noise ratio (SNR) and probability of the noise causing the threshold comparator to put out a binary one in a range bin, P_{N1}. The curves were obtained by simulating the signal-plus-noise distribution at the normal channel output. The simulation is discussed in Appendix E.

For a nonfluctuating target (Marcum's Case 0), the probability of the desired signal exceeding the threshold comparator level (P_{S1}, probability of a binary one in a range bin) for a single channel MTI canceller when averaged over all doppler frequencies can be approximated by (See Equation C-41):

$$P_{S1} = \int_{T}^{\infty} \frac{2}{\sqrt{2\Pi(\sigma^2+A^2/2)}} e^{\frac{-v^2}{2(\sigma^2+A^2/2)}} dv \qquad (D-24)$$

The integrand of Equation D-24 is the signal-plus-noise distribution at the threshold comparator input for a single channel MTI canceller (see Figure 3-35). Figure D-37 shows the probability of the desired signal-plus-noise exceeding the threshold comparator level (P_{S1}, probability of a binary one in a range bin). The probability of exceeding the threshold comparator level, P_{S1}, is shown as a function of the signal-to-noise ratio (SNR) and probability of the noise causing a binary one in a range bin, P_{N1}. The curves were obtained by simulating the signal-plus-noise distribution at the single channel MTI canceller output. The simulation is discussed in Appendix E.

A comparison of Figures D-36 and D-37 shows that for signal-to-noise ratios (SNR's) greater than zero dB the probability of the signal-plus-noise exceeding the threshold comparator level (P_{S1}, probability of a binary one in a range bin) is greater for the normal channel than for the single MTI channel. This would be expected when comparing the signal-plus-noise amplitude distributions at the integrator threshold comparator input. (See Figure 3-10 for the normal channel and Figure 3-35 for the single MTI channel).

The probability of a desired target return pulse train of 20 pulses causing the binary integrator to be be in state E_j can be determined by using a one-dimensional random walk with reflecting barriers model where levels 0 and 31 are the reflecting barriers. That is, the first and last rows of the Markov chain transition matrix are defined by (P_{S0}, P_{S1}, 0 ....) and (0,...0, P_{S0}, P_{S1}). The term P_{S0} is defined as the probability of the desired signal not exceeding the threshold comparator level (P_{S0}, probability of a binary zero in a range bin), and P_{S1} is defined as the probability of the desired signal exceeding the threshold comparator level (P_{S1}, probability of a binary one in a range bin). The actual probability of the desired pulse train causing the binary integrator to be in state E_j for a given signal-to-noise ratio is given by:

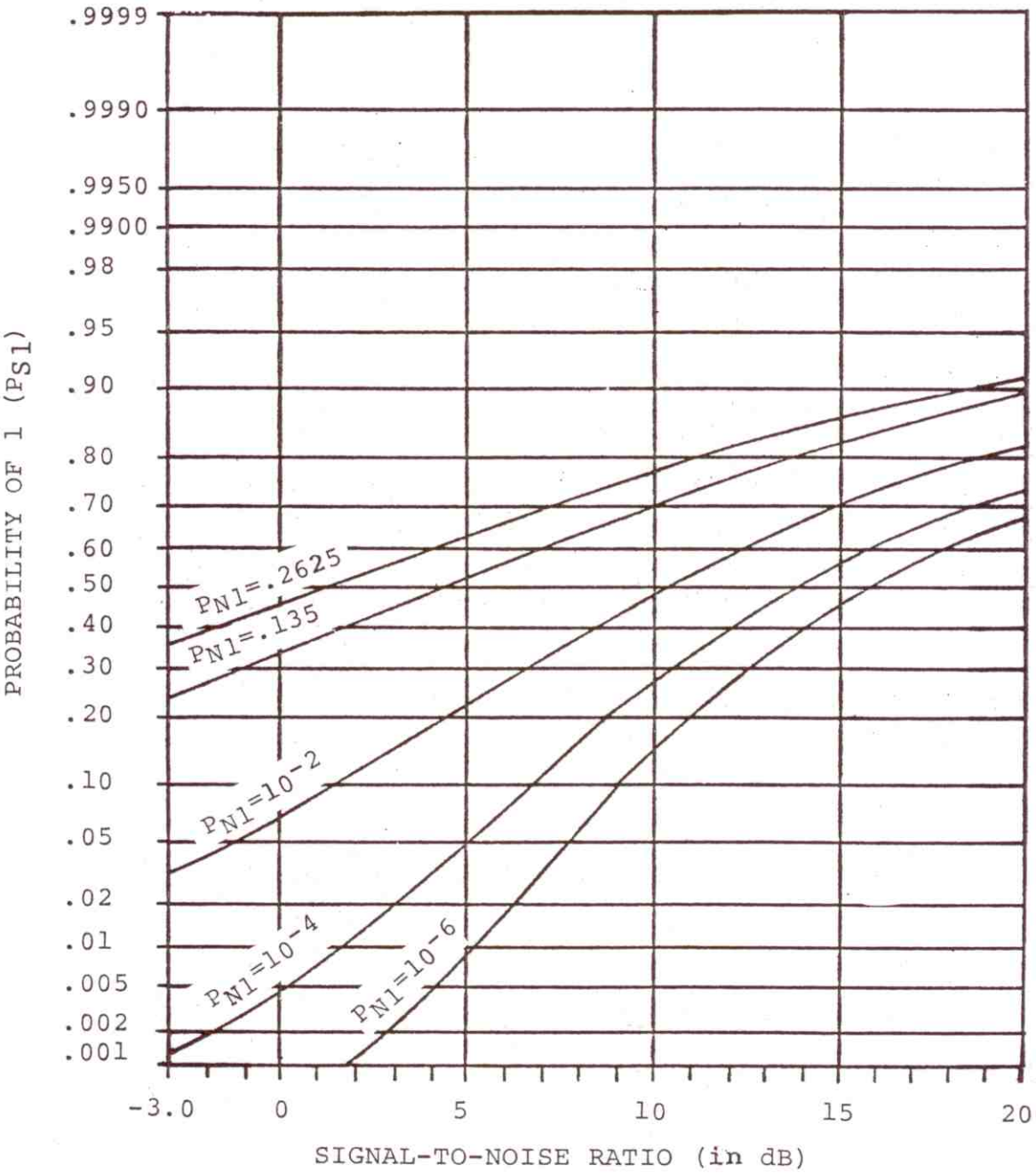

Figure D-37. Probability of 1 at the Threshold Comparator Output as a Function of the Signal-to-Noise Ratio at the Threshold Comparator Input for a Single Channel MTI Canceller

$$P_{sj} = \frac{\sum_{k=1}^{N} P_{ij}^{(k)}}{\sum_{j=1}^{\rho} \sum_{k=1}^{N} P_{ij}^{(k)}} \qquad \text{(D-25a)}$$

where:

$$P_{ij}^{(k)} = \frac{(p/q) - 1}{(p/q)^{\rho} - 1} \left(\frac{p}{q}\right)^{j-1} + \frac{2p}{\rho} \sum_{r=1}^{\rho-1} \frac{x_i^{(r)} y_j^{(r)} [2\sqrt{pq} \cos \pi r/\rho]^k}{1 - 2\sqrt{pq} \cos \pi r/\rho} \qquad \text{(D-25b)}$$

and

$$x_i^{(r)} = \left(\frac{q}{p}\right)^{i/2} \sin \frac{\pi r i}{\rho} - \left(\frac{q}{p}\right)^{(i+1)/2} \sin \frac{\pi r (i-1)}{\rho} \qquad \text{(D-25c)}$$

$$y_j^{(r)} = \left(\frac{p}{q}\right)^{j/2} \sin \frac{\pi r j}{\rho} - \left(\frac{p}{q}\right)^{(j-1)/2} \sin \frac{\pi r (j-1)}{\rho} . \qquad \text{(D-32d)}$$

ρ = Number of states (function of counter level sequence)

$q = P_{S0}$ = Probability of 0 at threshold comparator output

$p = P_{S1}$ = Probability of 1 at threshold comparator output

N = Number of desired signal pulses in target return pulse train

The values for P_{S1} as a function of signal-to-noise ratio are obtained from Figure D-36 for the normal channel and Figure D-37 for the single MTI channel, and $P_{S0} = 1 - P_{S1}$. The term $P_{ij}^{(k)}$ is defined as the probability of a transition from state E_i to state E_j in exactly k steps. In other words, $P_{ij}^{(k)}$ is the conditional probability of entering state E_j at the kth step given the initial state is E_i. Equation D-25b was obtained from Feller (1968).

TABLE D-6 shows the probability of the FAA modified integrator being in state E_j for a desired target return pulse train of 20 pulses, given that the initial state, E_i, was state 1. The table shows the probability of the

TABLE D-6

PROBABILITY OF DESIRED SIGNAL TARGET RETURN PULSE TRAIN OF 20 PULSES CAUSING THE FAA MODIFIED INTEGRATOR TO BE IN STATE E_j

State E_j	Counter Level	$P_{S1} = .600$	
		P_{sj}	ΣP_{sj}
1	0	.147409993+000	.147409993+000
2	1	.177353622+000	.324763614+000
3	2	.156627014+000	.481390628+000
4	4	.136325570+000	.617716198+000
5	8	.122056103+000	.739772301+000
6	16	.118857942+000	.858630243+000
7	31	.141369757+000	.100000000+001

State E_j	Counter Level	$P_{S1} = .800$	
		P_{sj}	ΣP_{sj}
1	0	.333096427-001	.333096427-001
2	1	.833176873-001	.116627330+000
3	2	.836663318-001	.200293662+000
4	4	.859261801-001	.286219842+000
5	8	.984266549-001	.384646497+000
6	16	.160277434+000	.544923930+000
7	31	.455076070+000	.100000000+001

State E_j	Counter Level	$P_{S1} = .995$	
		P_{sj}	ΣP_{sj}
1	0	.505040409-003	.505040409-003
2	1	.505040408-001	.510090813-001
3	2	.505040413-001	.101513123+000
4	4	.505041066-001	.152017229+000
5	8	.505190671-001	.202536296+000
6	16	.537338534-001	.256270150+000
7	31	.743729850+000	.100000000+001

desired signal being in state E_j as a function of the probability of the desired signal exceeding the threshold comparator level (P_{S1}) of .6, .8, and .995. The initial state, E_i, of 1 was chosen since for a probability of the noise exceeding the threshold comparator level (P_{N1}) of .135 the integrator is in state 1 with a probability of .8439 (see TABLE D-4).

The signal processing of the ASR-7 binary integrator was simulated to investigate the tradeoffs to the desired signal in suppressing asynchronous interference. Both the normal and single MTI channel signal processing was simulated. A detailed discussion of the simulation model is given in Appendix E. A simulated ASR-7 enhancer output for a desired target return pulse train of 20 pulses without noise present is shown in Figures D-38 and D-39 for the conventional ASR-7 enhancer and the FAA modified ASR-7 enhancer respectively. A comparison of Figures D-38 and D-39 shows that the FAA Modified ASR-7 enhancer provides a significant improvement in signal enhancement, target azimuth shift, and angular resolution.

Figures D-40 through D-43 show simulated radar performance of the FAA modified enhancer for the normal channel as a function of the signal-to-noise ratio (SNR). The desired target return pulse train consists of 20 pulses. Each figure shows the simulated radar output with the enhancer off (unintegrated) and enhancer on (integrated). Figure D-40, SNR = 3 dB; and Figure D-41, SNR = 5 dB; show that with the enhancer off the desired signal is down in the noise. However, when the enhancer is on the signal is pulled out of the noise by the binary enhancer. This should be expected since the probability of the desired signal exceeding the threshold comparator level, P_{S1}, is greater than the probability of the noise exceeding the threshold comparator level, P_{N1} = .135, for SNR's of 3 and 5 dB (see Figure D-36).

Figures D-44 through D-46 show simulated radar performance of the FAA modified enhancer for the single MTI channel (mode 1 and 2 CASC) as a function of the signal-to-noise ratio (SNR) with the enhancer off (unintegrated) and on (integrated). A comparison of Figures D-40 with D-44 and D-42 with D-45 (same SNR for normal and MTI channels) shows that the signal enhancement is greater for the normal channel than for the MTI channel. This should be expected since the probability of the desired signal exceeding the threshold comparator level, P_{S1}, is greater for the normal channel than for the single MTI channel for a given SNR. (Compare Figures D-36 and D-37.)

The target azimuth shift due to integration is given by Equation D-12. Using Figure D-39 and Equation D-12, the FAA modified binary enhancer causes a target azimuth shift of approximately .179 degrees. The feedback integrator caused a target azimuth shift of approximately .900 degrees. Therefore, the FAA modified binary enhancer results in a significant improvement in target azimuth shift over the feedback integrator.

The property of the radar to distinguish between targets is called resolution. Using Figure D-39 and Equation D-13, the use of the FAA modified binary enhancer does not cause any loss in target angular resolution. It was

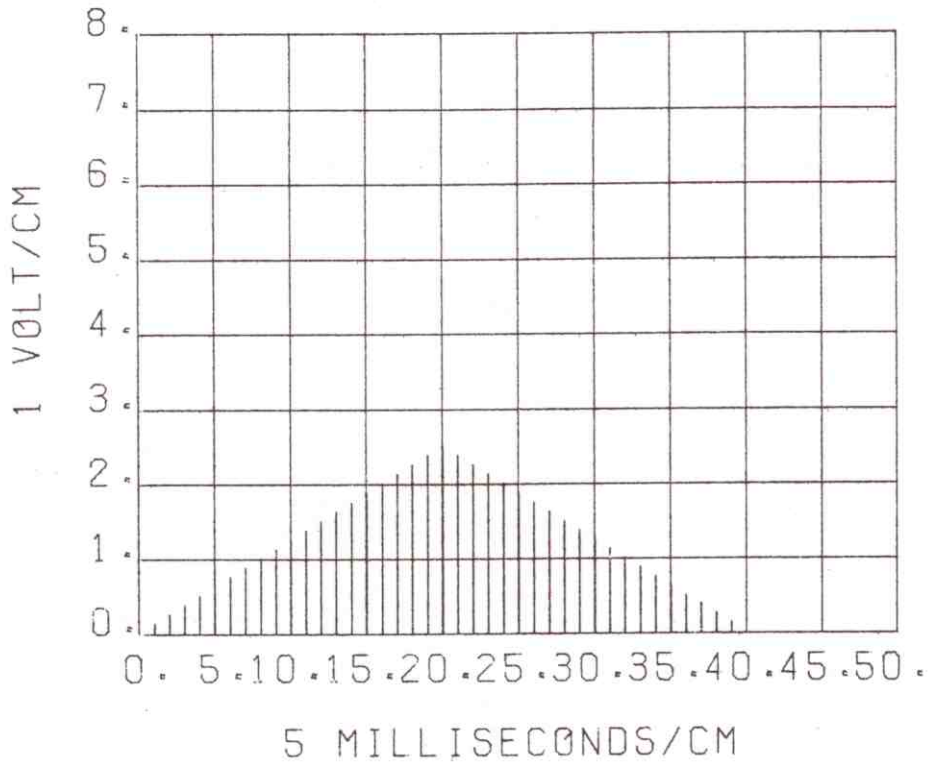

Figure D-38. Simulated Binary Integrator Output for Target Return Pulse Train (ASR-7, AN/GPN-12)

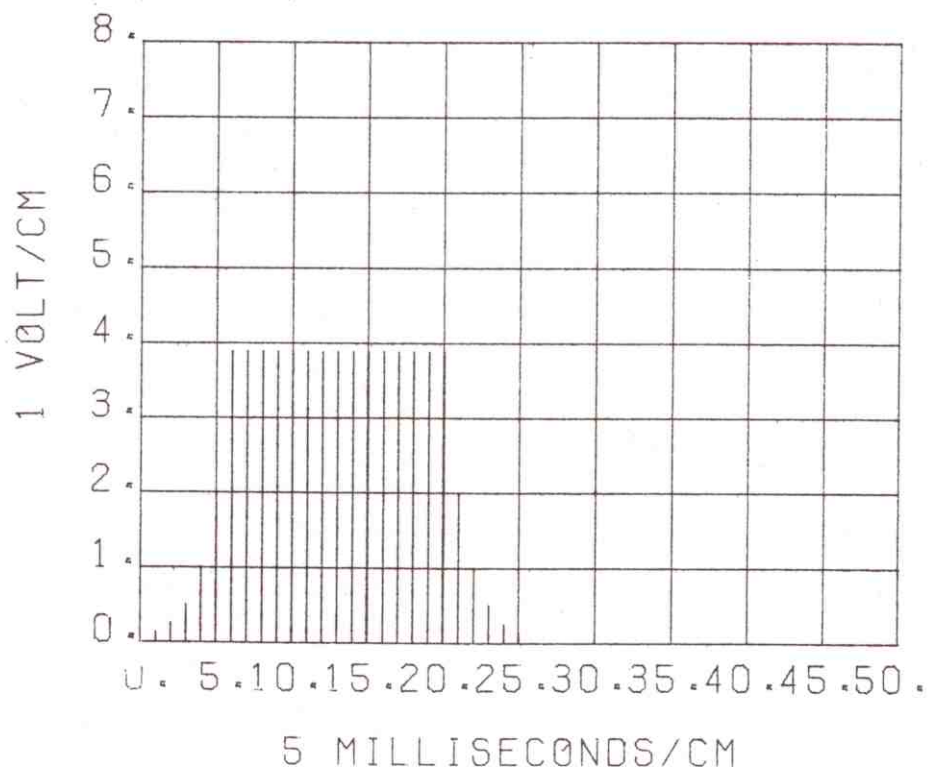

Figure D-39. Simulated FAA Modified Binary Integrator Output for Target Return Pulse Train (ASR-7)

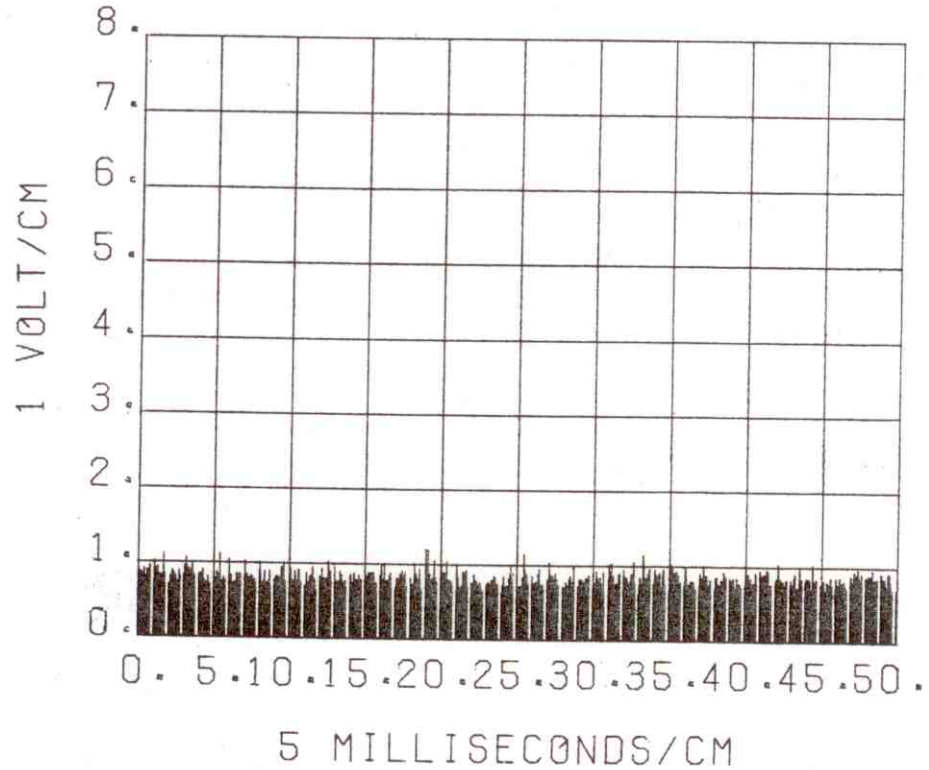

Figure D-40a. Simulated Normal Channel Unintegrated Target Return Pulse Train for a SNR = 3dB

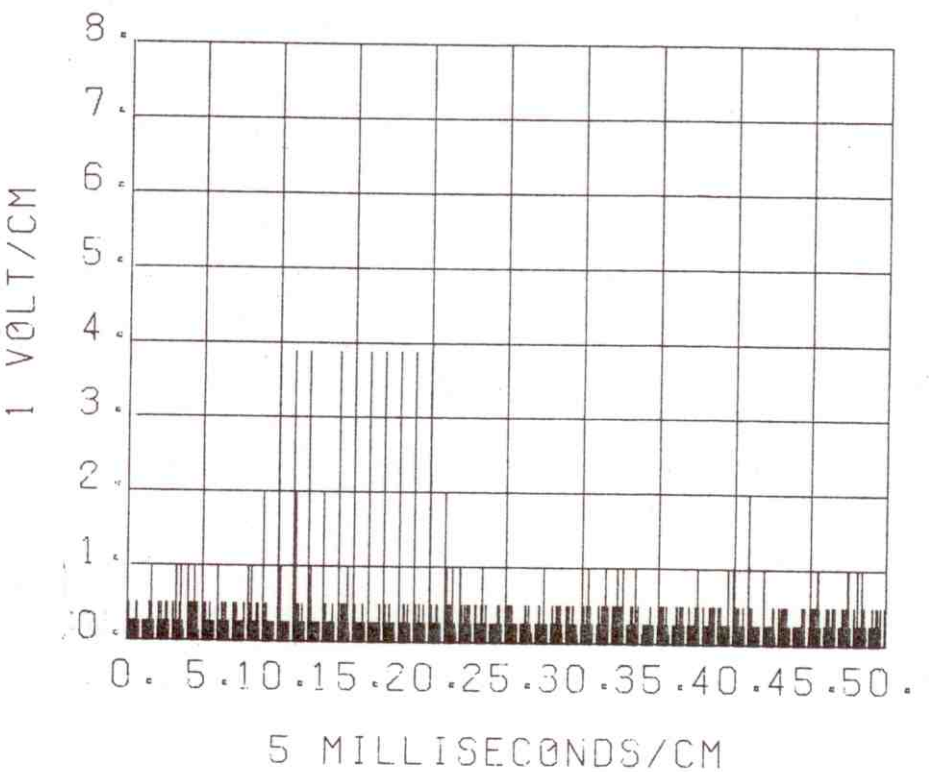

Figure D-40b. Simulated Normal Channel Integrated Target Return Pulse Train for a SNR = 3dB

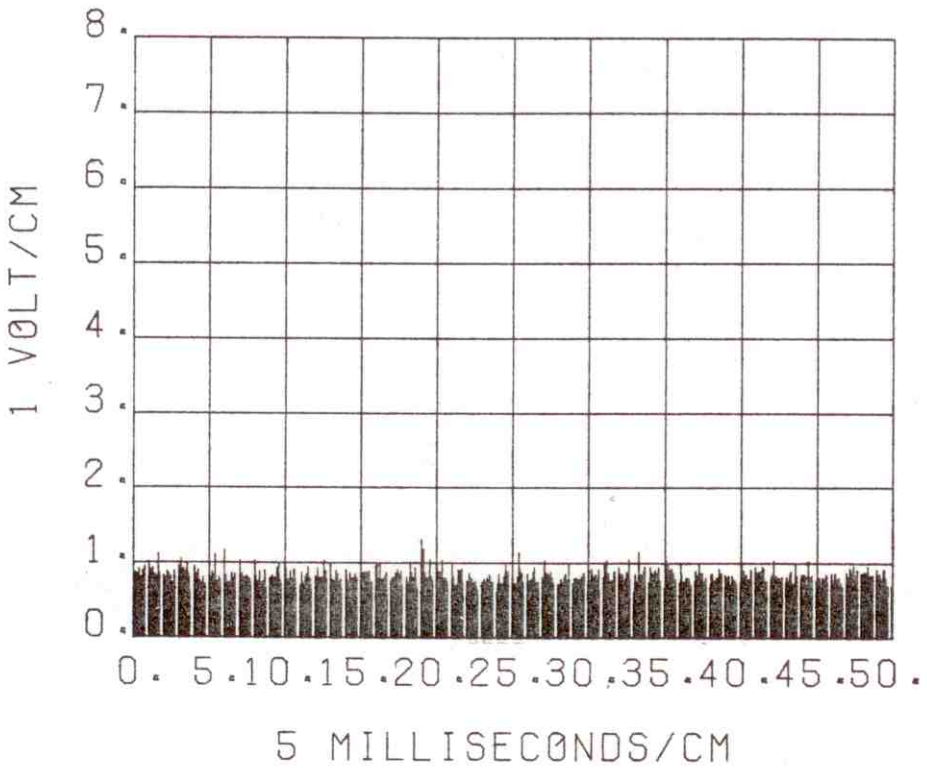

Figure D-41a. Simulated Normal Channel Unintegrated Target Return Pulse Train for a SNR = 5dB

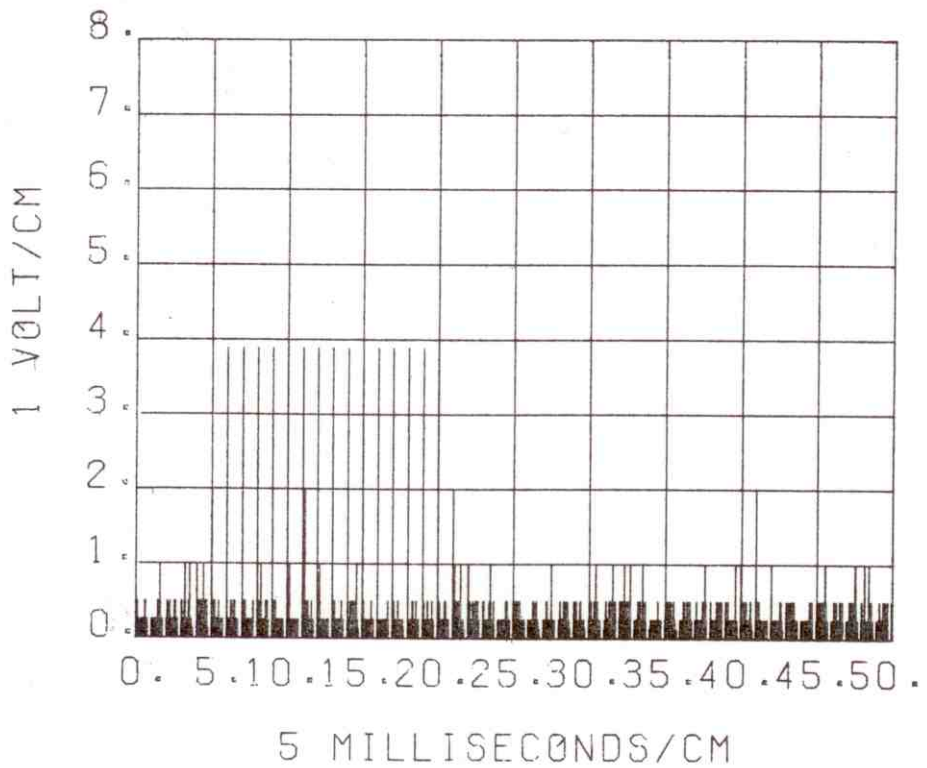

Figure D-41b. Simulated Normal Channel Integrated Target Return Pulse Train for a SNR = 5dB

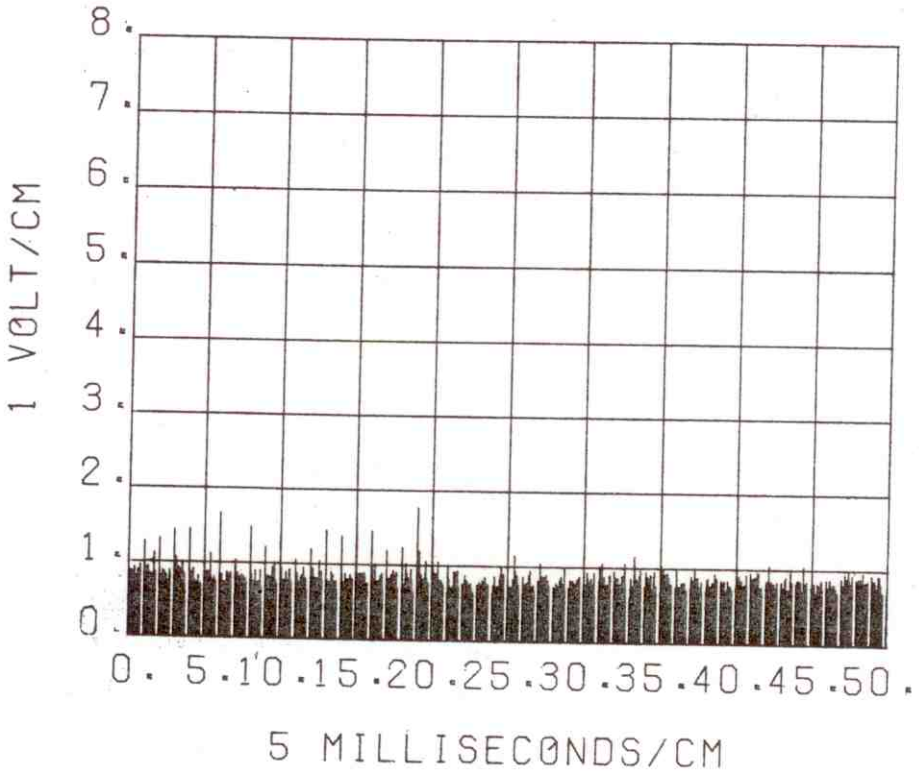

Figure D-42a. Simulated Normal Channel Unintegrated Target Return Pulse Train for a SNR = 10dB

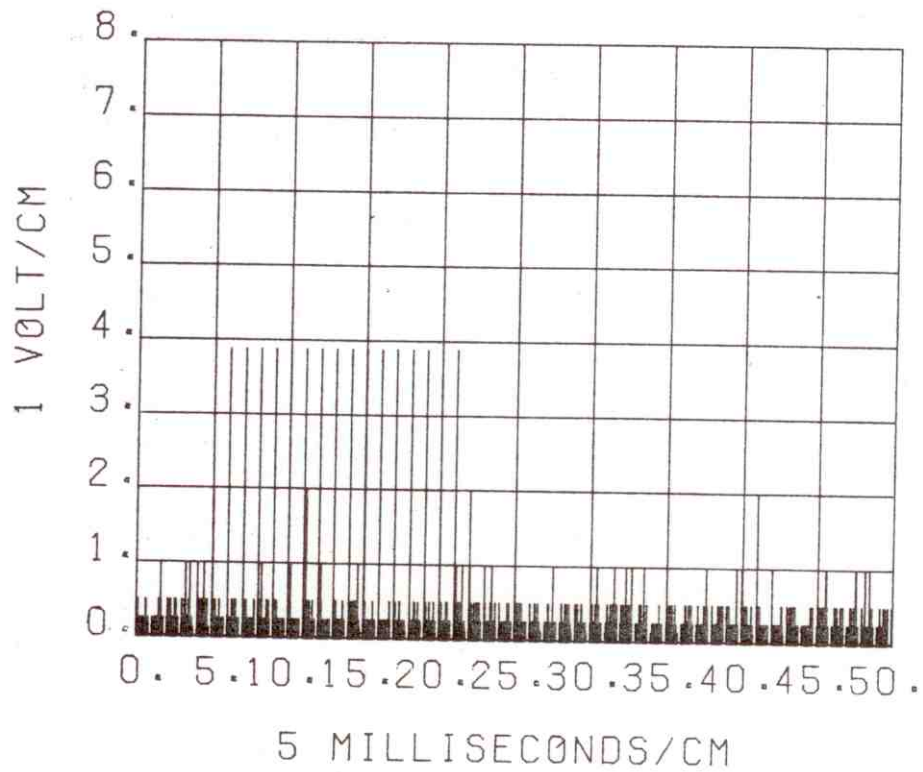

Figure D-42b. Simulated Normal Channel Integrated Target Return Pulse Train for a SNR = 10dB

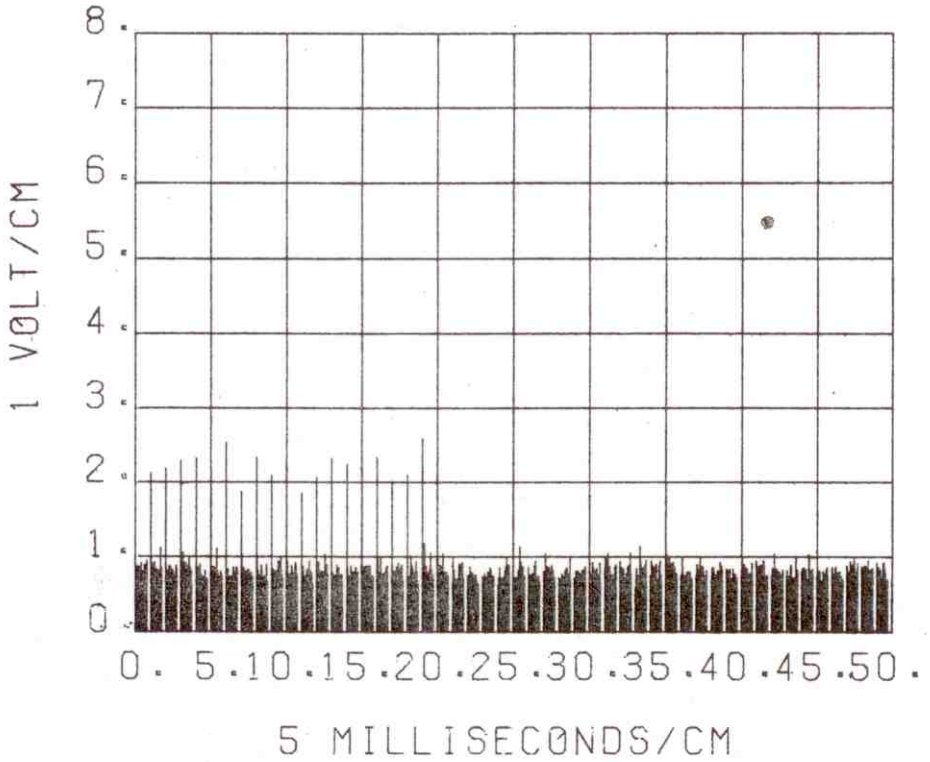

Figure D-43a. Simulated Normal Channel Unintegrated Target Return Pulse Train for a SNR = 15dB

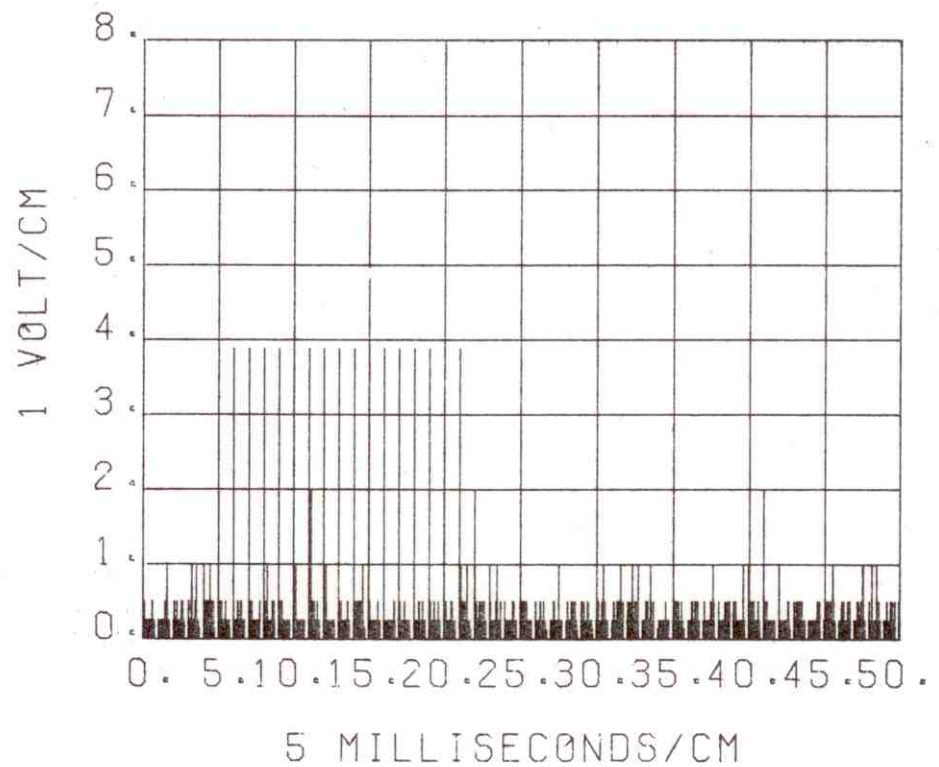

Figure D-43b. Simulated Normal Channel Integrated Target Return Pulse Train for a SNR = 15dB

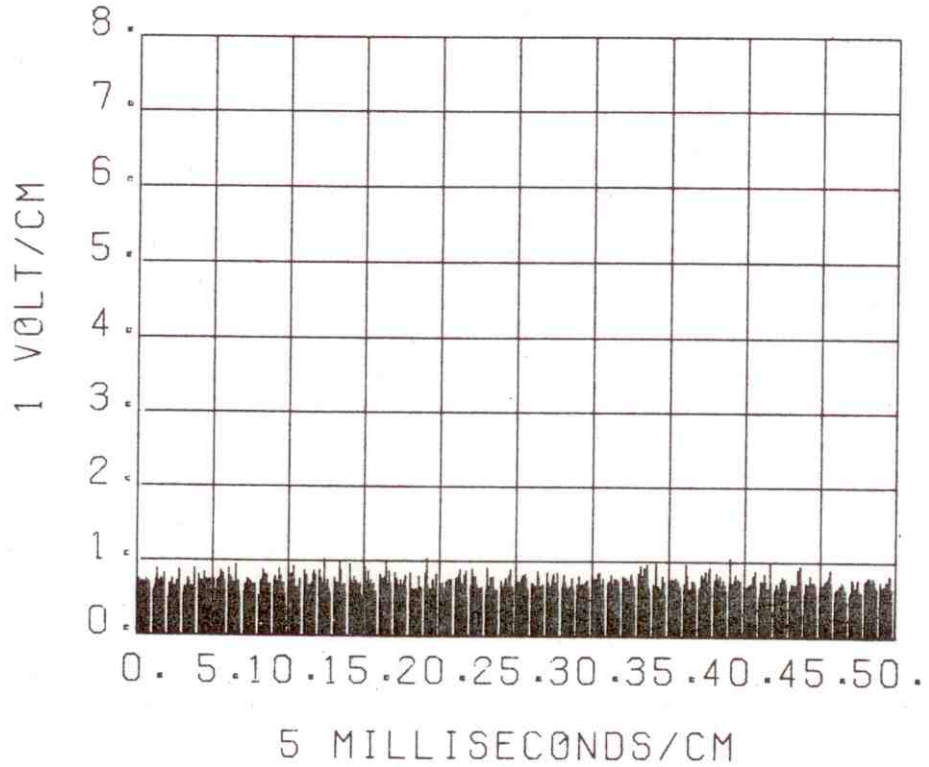

Figure D-44a. Simulated MTI Channel (Mode 1 & 2 CASC) Unintegrated Target Return Pulse Train for a SNR = 3dB

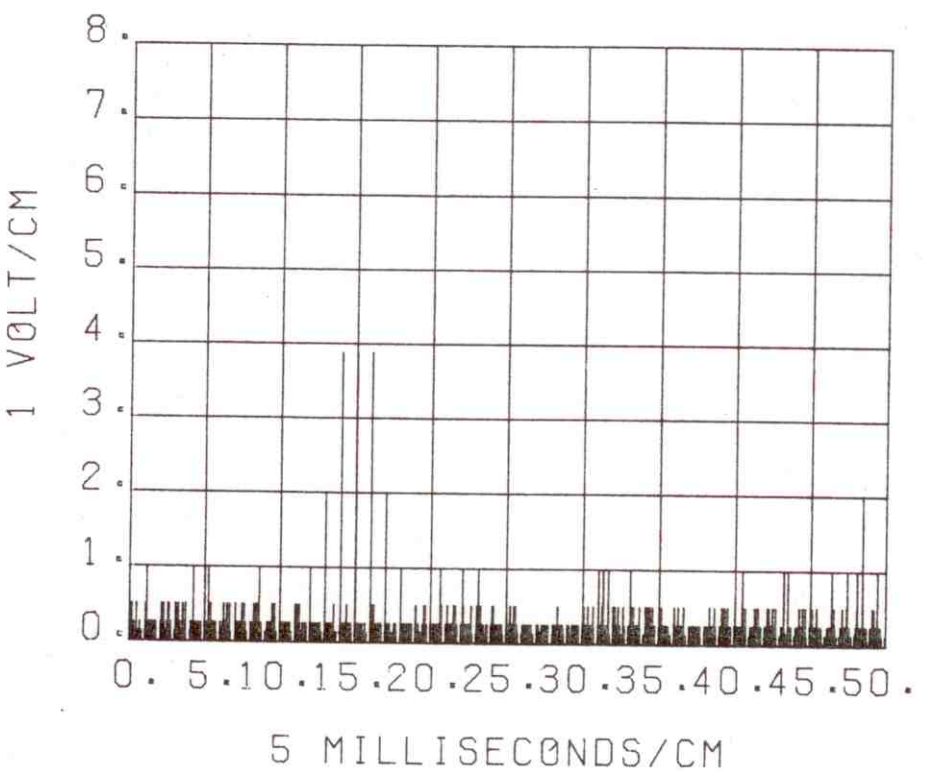

Figure D-44b. Simulated MTI Channel (Mode 1 & 2 CASC) Integrated Target Return Pulse Train for a SNR = 3dB

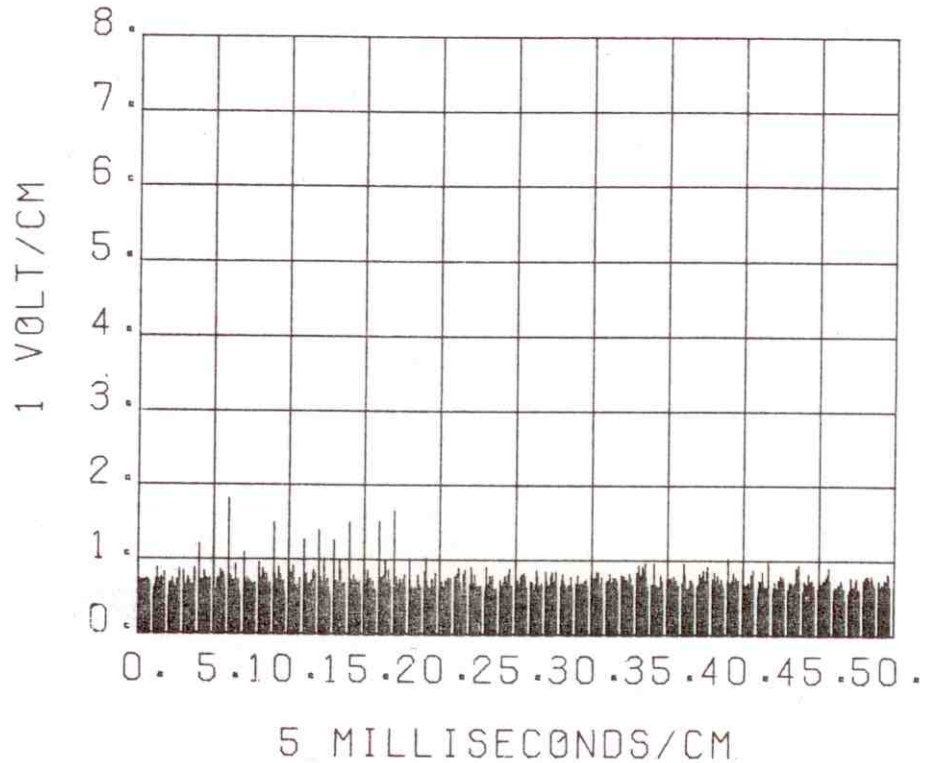

Figure D-45a. Simulated MTI Channel (Mode 1 & 2 CASC) Unintegrated Target Return Pulse Train for a SNR = 10dB

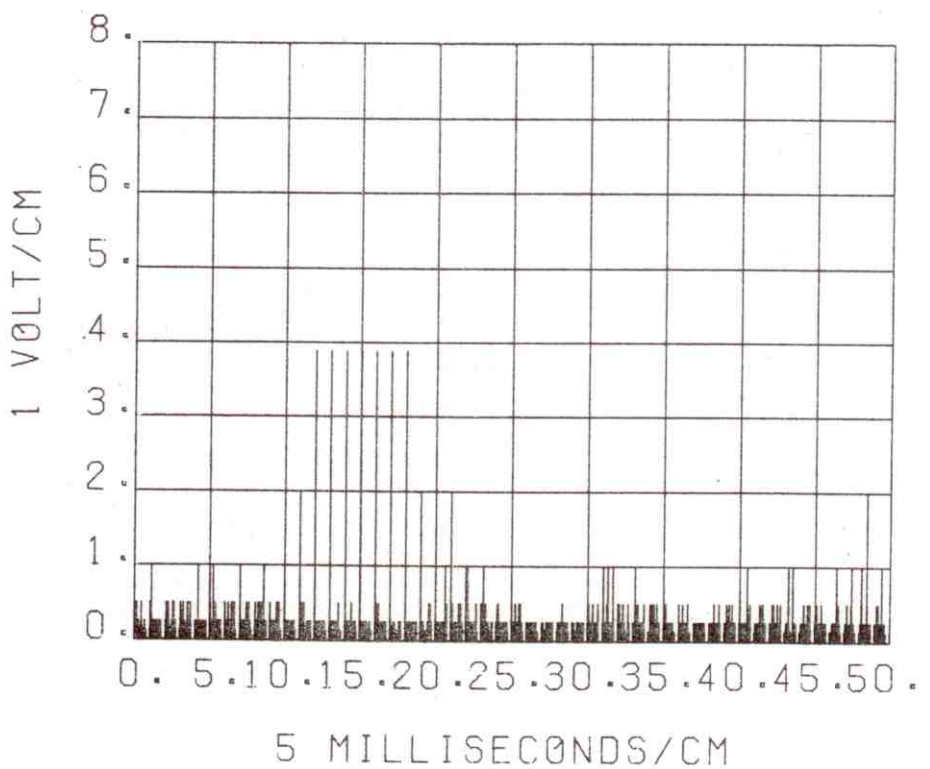

Figure D-45b. Simulated MTI Channel (Mode 1 & 2 CASC) Integrated Target Return Pulse Train for a SNR = 10dB

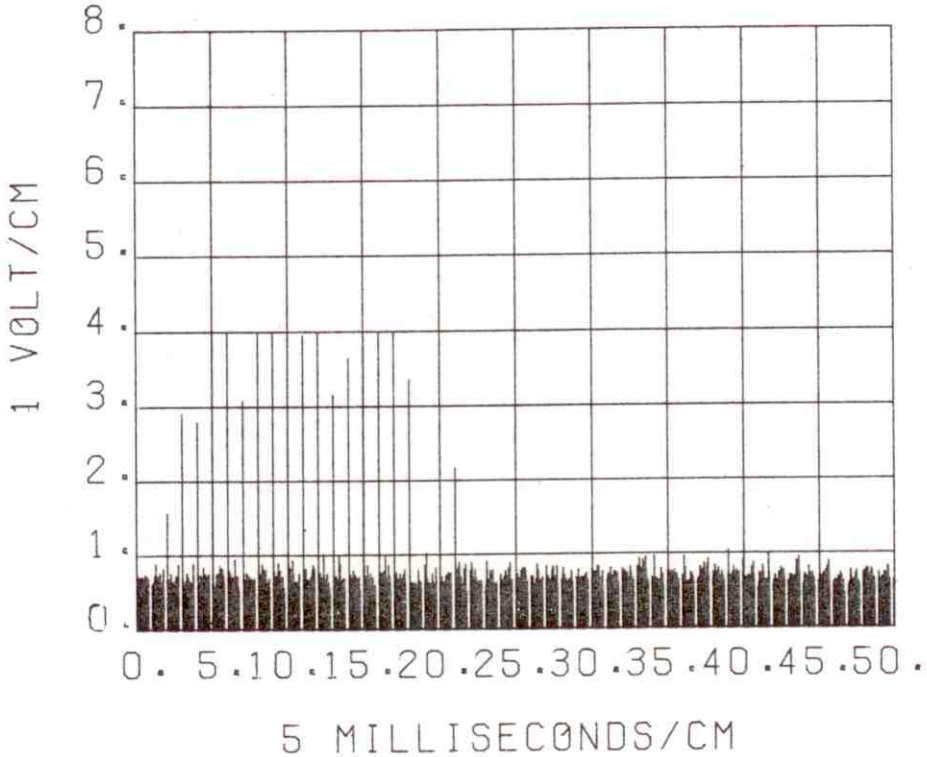

Figure D-46a. Simulated MTI Channel (Mode 1 & 2 CASC) Unintegrated Target Return Pulse Train for a SNR = 20dB

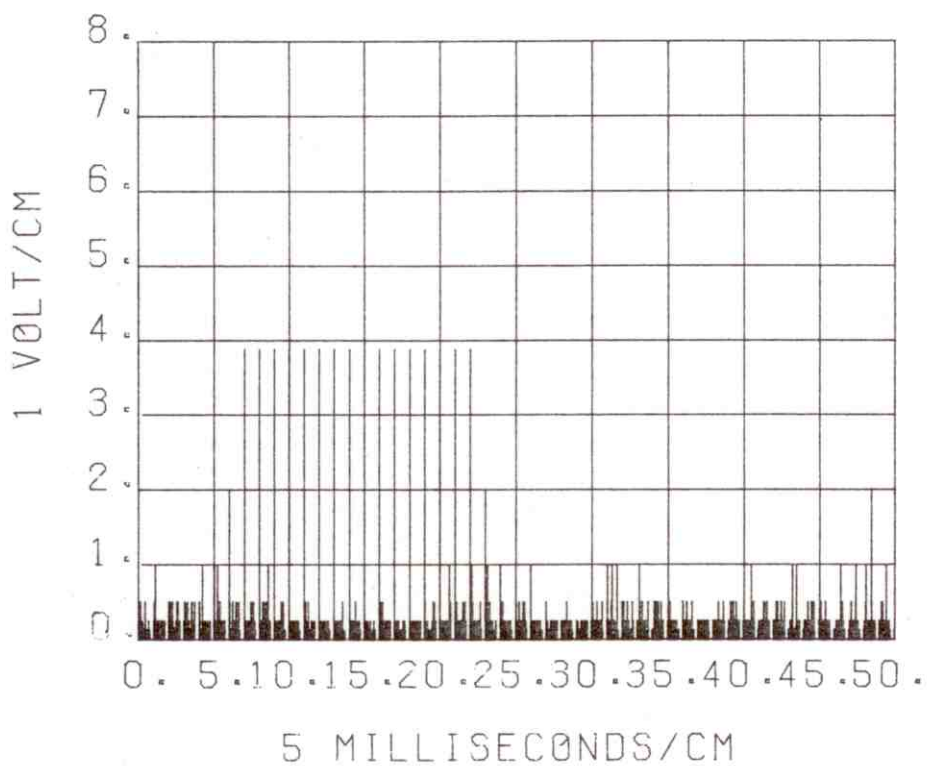

Figure D-46b. Simulated MTI Channel (Mode 1 & 2 CASC) Integrated Target Return Pulse Train for a SNR = 20dB

previously shown that the feedback integrator caused between 1.2 and 1.5 degrees loss in angular resolution.

Interference

The capability of the binary integrator in the ASR-7 to suppress asynchronous interference was also investigated using the radar simulation model (see Appendix E). Three interfering radar sources were simulated: ASR-5, ASR-8, and the AN/FPS-90. Figures E-3 through E-5 in Appendix E show the respective time waveforms simulated for each of the radar interfering sources.

For the normal radar channel, the probability of the interference, P_{ij}, appearing above the one volt peak noise level (enhancer state 8) can be expressed as:

$$P_{ij} = P_{n8} \cdot P_{I1} \cdot (1-e^{-\nu(\tau+RB_s)}) \qquad \text{(D-26)}$$

where:

P_{n8} = Probability of the noise causing the enhancer to be in level 8

P_{I1} = Probability of the interference exceeding the threshold comparator level setting

ν = Interfering pulse arrival rate, in pulses per second

τ = Interfering signal pulse width, in seconds

RB_s = Radar quantizer range bin sample time, in seconds

The probability of the noise causing the enhancer to be in level 8 is a function of the enhancer threshold comparator level setting, and the hit/miss sequence programmed in the enhancer. For the FAA modified enhancer and a probability of the noise exceeding the threshold comparator level (P_{N1}) of .135, the probability of the noise causing the enhancer to be in level 8 is .0005 (see TABLE D-4). For an ASR-8 interfering source (γ = 1040, τ = 0.6 μ sec, RB_s = .166 μ sec), the probability of the interference causing the enhancer to exceed level 8 (one volt level) is 3.98×10^{-7} assuming P_{I1} = 1. The value of P_{I1} is a function of the interference-to-noise ratio at the enhancer input and can be obtained using Figure D-36. Figure D-47a shows a simulated normal channel radar unintegrated output for three interference sources (ASR-5, INR = 10 dB; ASR-8, INR = 15 dB; and AN/FPS-90, INR = 20 dB), and a desired target signal-to-noise ratio of 15 dB. Figure D-47b shows for the same interference condition the radar output after integration. The asynchronous interference has been suppressed (compare Figure D-43b with D-47b).

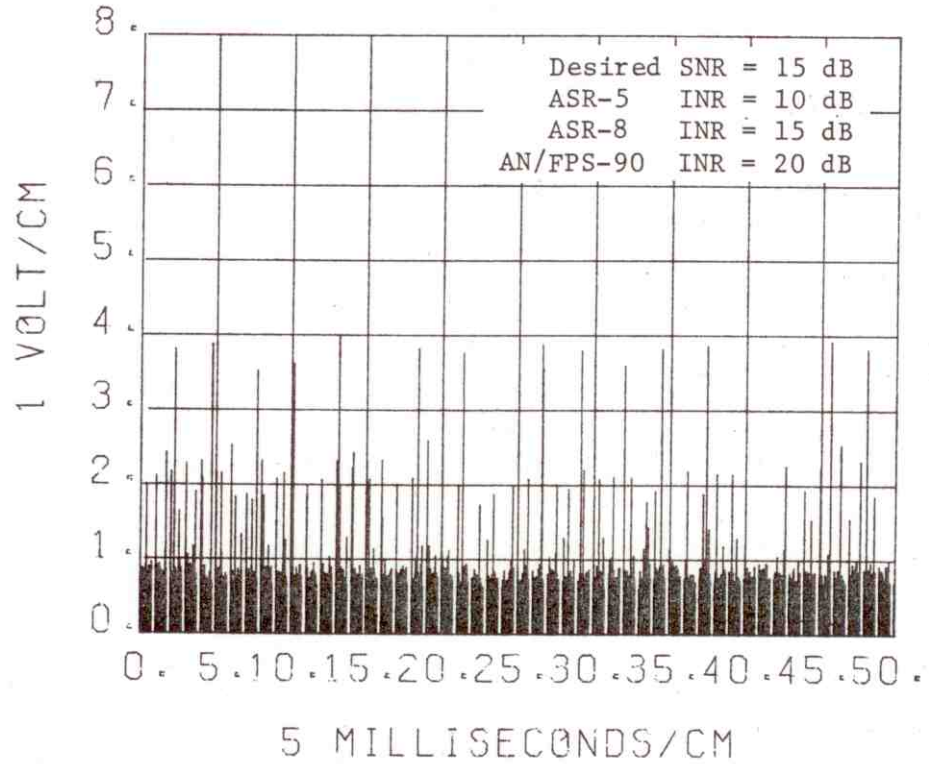

Figure D-47a. Simulated Normal Channel Unintegrated Radar Output with Interference

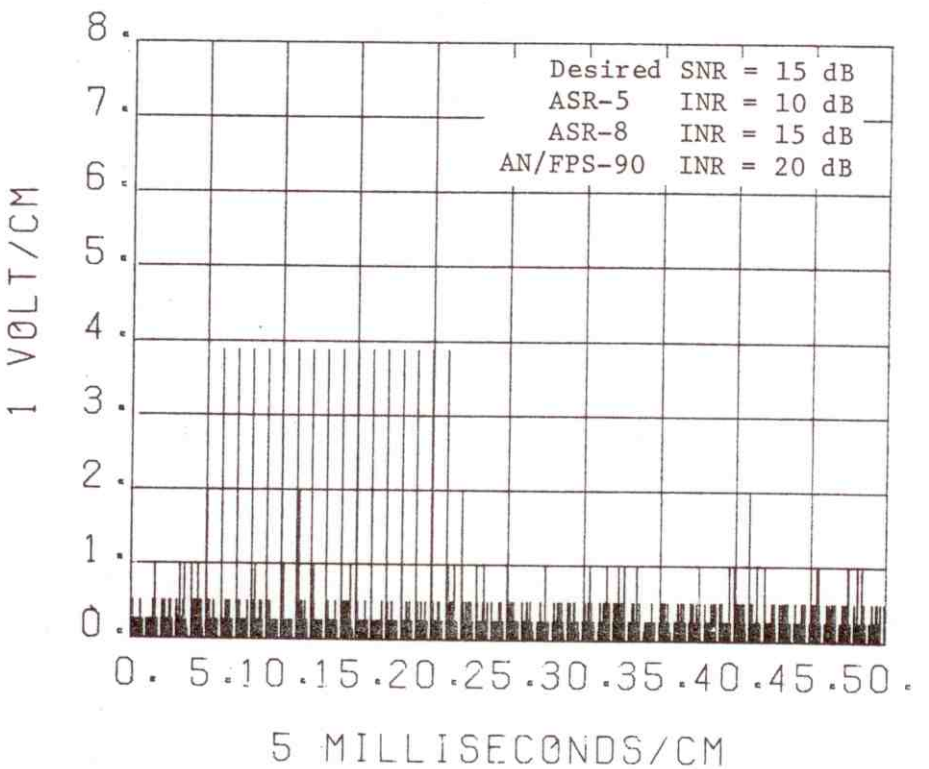

Figure D-47b. Simulated Normal Channel Integrated Radar Output with Interference

For the MTI channel, the analytical expression for the probability of the interference, P_{ij}, appearing above the one volt noise level (enhancer level 8) becomes complex. This is due to the fact that the MTI canceller transfer properties to asynchronous interference results in several synchronous interfering pulses at the MTI canceller output. (See Figures C-16 through C-20.) To assess the probability of the interference causing the enhancer to exceed level 8, all the combination of ways of exceeding level 8 must be considered along with the varying INR of the synchronous interfering pulses at the canceller output. Because of this, the best way of analyzing the capability of the enhancer to suppress asynchronous interference in the radar MTI channel is by simulation. Figure D-48a shows a simulated MTI channel radar unintegrated output for three interfering sources (ASR-5, INR = 10 dB; ASR-8, INR = 15 dB; and AN/FPS-90, INR = 20 dB), and a desired target signal-to-noise ratio (SNR) of 20 dB. Figure D-48b shows for the same interference condition the radar output after integration. The asynchronous interference has been suppressed (compare Figures D-46b with Figure D-48b).

In summary, the FAA modified binary enhancer has the capability of suppressing asynchronous interference with very little trade-offs in target azimuth shift, target angular resolution and desired target probability of detection. Asynchronous interference can be suppressed by the FAA modified enhancer by either adjusting the threshold comparator level setting, or by programming a hit/miss state sequence that will suppress the interference. Thus the FAA modified ASR-7 enhancer can be adjusted to optimize the radar desired signal performance in a variety of environmental conditions.

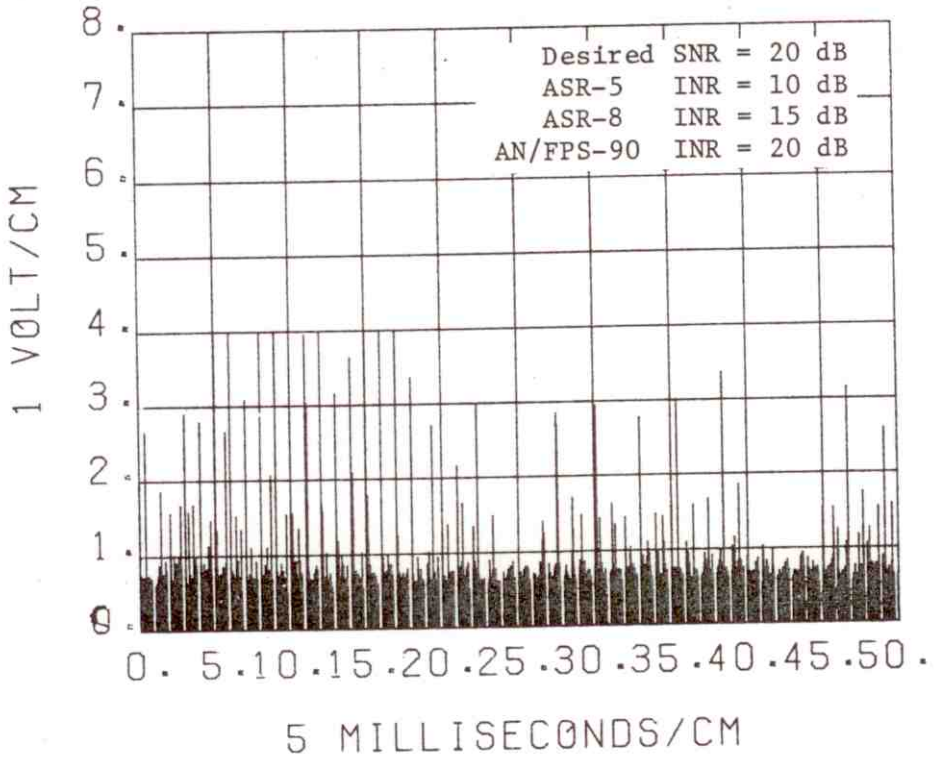

Figure D-48a. Simulated MTI Channel (mode 1 & 2 CASC)
Unintegrated Radar Output with Interference

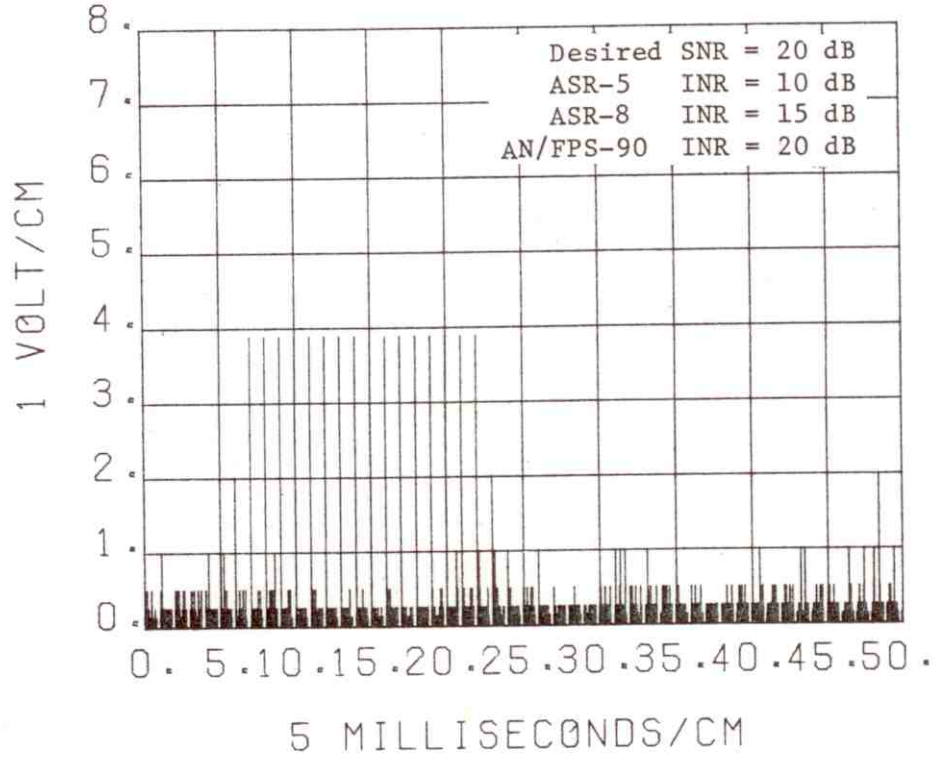

Figure D-48b. Simulated MTI Channel (mode 1 & 2 CASC)
Integrated Radar Output with Interference